Neurochem Res (2019) 44:683–691
DOI 10.1007/s11064-017-2418-2

ORIGINAL PAPER

Regulation of Neurotransmitter Release by Amyloid Precursor Protein Through Synapsin Phosphorylation

An Liu[1] · Ying Zhang[1] · Lifang Han[1] · Guiqin He[1] · Wei Xie[1] · Zikai Zhou[1] · Zhengping Jia[2,3]

Received: 30 May 2017 / Revised: 1 October 2017 / Accepted: 9 October 2017 / Published online: 19 October 2017

Abstract Abnormal processing of amyloid precursor protein (APP) and aggregation of the Aβ peptide are known to play a key role in the pathogenesis of Alzheimer disease, but the function of endogenous APP under normal physiological conditions remains poorly understood. In this study, we investigated presynaptic changes in APP knockout (KO) mice. We demonstrate that both sucrose-induced neurotransmission and synaptic depletion in response to high frequency stimulation are significantly enhanced in APP KO compared to wild type littermates. In addition, the level of phosphorylated forms of synapsins, but not total synapsins, is elevated in the KO mice. Furthermore, we show that the inhibition of L-type calcium channels normalizes phosphorylated synapsins and slows down the high frequency induced synaptic depletion in APP KO mice. These results suggest a new mechanism by which APP regulates synaptic vesicle dynamics through synapsin-dependent phosphorylation.

Keywords Alzheimer disease · Amyloid precursor protein · Synaptic depletion · Synapsin · Ca^{2+} channel

An Liu and Ying Zhang contributed equally to this work.

✉ Zhengping Jia
zhengping.jia@sickkids.ca

[1] Institute of Life Sciences, The Key Laboratory of Developmental Genes and Human Disease, Jiangsu Co-innovation Center of Neuroregeneration, Southeast University, Nanjing 210096, China

[2] Neurosciences & Mental Health, the Hospital for Sick Children, 555 University Ave., Toronto, ON M5G 1X8, Canada

[3] Department of Physiology, Faculty of Medicine, University of Toronto, Toronto, ON, Canada

Introduction

Alzheimer disease (AD) is the most common form of dementia that affects millions worldwide and imposes enormous economic and social burden on the affected individuals and our society. However, our ability to treat this disease is limited due to incomplete understanding of the fundamental mechanisms underlying the pathogenic process of this disorder. One of the key theories is the amyloid-β (Aβ) hypothesis that posits that the accumulation of Aβ and the formation of Aβ oligomers impairs neuronal function, including synaptic regulation, leading to memory loss and, ultimately, to dementia [1–3]. Aβ peptide is a proteolytic fragment of amyloid precursor protein (APP), whose mutations are linked to AD patients [4–6]. Although it is agreed that the abnormal processing of APP and thus aggregation of the Aβ peptide is a key player in the pathogenesis of AD, the function of APP under normal physiological conditions remains poorly defined.

Several studies have shown that APP plays important roles in neuronal development. In vitro studies indicate that APP is expressed in the lamellipodia of neuronal growth cones [7, 8] and affects axonal outgrowth through Rac1, a key mediator of actin reorganization [9]. Accordingly, axonal connectivity in APP knockout (KO) mice is mildly impaired in the forebrain commissures [10] and retinotectal system [11, 12]. APP also regulates dendritic complexity and spine density. Lack of APP or engineered APP mutations within the C terminus decrease the dendritic complexity and spines in the hippocampal CA1 neurons in vitro [13–15] and in vivo [13, 16]. APP KO cortical or hippocampal neurons also have reduced spine densities [13, 14, 17, 18]. It is important to note that some of these changes in APP KO mice are age-dependent.

In neurons APP is also localized at the synapse suggesting a role in synaptic transmission and plasticity. In patients with AD, synaptic dysfunction is highly correlated with cognitive decline [19], and Aβ oligomers from patients can directly impair synaptic plasticity and memory in mice [1, 20]. Indeed, APP KO mice exhibited age-dependent impairments in long-term potentiation (LTP) and hippocampus-dependent behaviour, including spatial learning in the Morris water maze [21, 22], consistent with age-dependent reductions in spine defects in these mice [23]. In conditional double KO mice lacking both APP and APLP2, another member of the APP family, strong deficits in the dendritic spines, LTP and memory are present in young mice, suggesting an overlapping and compensatory interactions among APP and its family members [17].

In addition to postsynaptic regulation, APP is implicated in presynaptic function. In particular, APP and APLP2 double conditional KO mice show impairments in paired-pulse facilitation (PPF) and the early phase of post-tetanic potentiation, both of which are thought to be of presynaptic origin [17]. In addition, responses to repetitive stimulation of the Schaffer collaterals are altered in neonatal the double KO mice [24]. However, underlying molecular mechanisms responsible for these presynaptic alterations remain unknown.

In this study, we investigated the role of APP in presynaptic function using APP KO mice. We showed that APP KO mice (4–5 weeks-old) were altered in sucrose induced release as well as synaptic depression in response to sustained high frequency stimulation. In addition, we showed that the level of phosphorylated synapsin, a key presynaptic regulator, was significantly elevated in APP KO mice and this elevation was reduced by the L-type calcium channel blocker nifedipine. Similarly, the enhanced synaptic depletion in APP KO mice was rescued by nifedipine. These results suggest that APP regulates neurotransmitter release through a synapsin-dependent mechanism.

Materials and Methods

Mice

APP KO mice were obtained from Model Animal Research Center of Nanjing University and genotyped using PCR techniques as previously described [25]. All mice were maintained and used according to experimental protocols approved by the Animal Care Committee at the Hospital for Sick Children (Toronto, Canada) and Southeast University (Nanjing, China). The age of the mice used in this study was between 4 and 5 weeks. This age was chosen because we aimed to investigate the roles of APP in presynaptic function without potential confounding effects of postsynaptic changes (e.g., spine deficits), which are present in relatively aged APP KO mice.

Antibodies, Chemicals and Other Reagents

Primary and secondary antibodies include: Rabbit polyclonal anti-Synapsin1 (Bioworld, Cat#BS4116), Rabbit polyclonal anti-p-CaMKII (Thr 286) (Cell signaling technology, Cat#12716), Rabbit polyclonal anti-p-Synapsins (Cell signaling technology, Cat#2311), Rabbit polyclonal anti-Actin (Proteintech, Cat#20536-1-AP), Goat polyclonal anti-NRXN1α (LifeSpan BioSciences, Cat#LS-C61771), Mouse monoclonal anti-GAPDH (Proteintech, Cat#60008-1-lg), Goat anti-rabbit (Genscript, Cat#A00098), Alexa Fluor 488 donkey anti-goat IgG (Jackson ImmunoResearch, Cat#705-546-147), Alexa Fluor 555 donkey anti-rabbit IgG (Thermo-Fisher, Cat#A-31570). Drugs include: Picrotoxin (Sigma-Aldrich, Cat#R284556), D-APV (Tocris, Cat#0106), NBQX (Sigma-Aldrich, Cat#N183), Diamond Antifade Mountant (Thermo-Fisher, Cat#P36965), Nifedipine (Sigma-Aldrich, Cat#N7634).

Slice Electrophysiology

All the electrophysiological recordings were carried out as previously described [26–28]. Briefly, the mouse brains from wild type (WT) and APP KO littermates (4–5 week old, sex balanced) were quickly removed, and sagittal 360 μm hippocampal slices were prepared in ice-cold artificial cerebrospinal fluid (ACSF) saturated with 95% O_2/5% CO_2. ACSF contained (in mM): 120.0 NaCl, 3.0 KCl, 1.2 $MgSO_4$, 1.0 NaH_2PO_4, 26.0 $NaHCO_3$, 2.0 $CaCl_2$, and 11.0 D-glucose. The slices were recovered at 28 °C for at least 2 h before a single slice was transferred to a submersion chamber perfused with 95% O_2/5% CO_2 saturated ACSF. For EPSC recording, 100 μM picrotoxin were used to block inhibitory response, and 50 μM D-APV and 10 μM NBQX were used to record IPSC response. Hippocampal CA1 neurons were visualized using an infrared differential interference contrast microscope (Zeiss Axioscope or Olympus X51). Synaptic response was evoked at 0.1 Hz for whole-cell currents, and recorded with glass pipettes (3–4 MΩ) filled with the intracellular solution containing (in mM) 130.0 $CsMeSO_4$, 5.0 NaCl, 1 $MgCl_2$, 0.05 EGTA, 10.0 HEPES, 3.0 Mg-ATP, 0.3 Na_3GTP, and 5.0 QX-314 (pH 7.5) (280–300 mOsm) at − 65 mV. For the synaptic depletion experiments, responses were evoked by stimulating the Schaffer collaterals at 5 Hz for 180 s. For the sucrose puff experiments, after the CA1 neuron was clamped at − 65 mV, sucrose-induced current was evoked by a fast puff (70 s for EPSC, 3 s for IPSC) delivered through a pipette (3–5 MΩ) filled with ACSF containing 100 μM picrotoxin (for EPSC) or 50 μM D-APV plus 10 μM NBQX (for IPSC), and 500 mM sucrose by using

the PV830 Pneumatic Picopump (WPI). All recording data acquisition and analysis were done using the pCLAMP 10.2 (Axon Instruments). n in all recording figures represents the number of slices/neurons and normally only one or two slices from each animal were used. The precise numbers of number of slices/neurons and animals are indicated in the figure legend.

Immunohistochemistry of Brain Sections

The procedures for brain processing and immunohistochemistry were described previously [28]. Mice were anesthetized by 10% chloral hydrate and subjected to cardiac perfusion with 0.1 M phosphate-buffered saline (PBS) followed by 4% paraformaldehyde. The brain was then dissected and further fixed in 4% PFA/PBS for 24 h, and then transferred to 30% sucrose/PBS solution for another 24 h. The brain was embedded in O.C.T. compound, frozen in liquid nitrogen and stored at − 80 °C, before being sliced to 25 µm coronal crystat sections at − 20 °C (Leica CM1950). Sections were washed with PBS, permeabilized by 0.1% Triton X-100 in PBS for 2 h, blocked with 10% fetal bovine serum for 1 h, and incubated with the NRX1α/p-Synapsin1 antibodies overnight at 4 °C followed by appropriate secondary antibodies at 37 °C for 2 h. After washing, the stained coverslips were mounted with the ProLong Diamond Antifade mounting medium for image collections. Confocal images were obtained at room temperature on Zeiss LSM 700 at 2048 × 2048 pixels using Zeiss 5× (NA 0.15, dry) objective with the same settings and configurations for all samples within each experiment. All images were initially acquired through the Zen 2010 software (Zeiss). AimImageBrowser software (Zeiss) was used to adjust the image brightness/contrast and extract a subregion. All measurements were performed using the ImageJ software (NIH).

Western Blot Analysis

Whole brain protein lysates were prepared from 4 to 5 week-old APP KO and WT littermates as previously described [26, 29]. One mouse brain was homogenized in a Dounce homogenizer with 1.5 ml ice-cold lysis buffer containing (in mM): 20 Tris–HCl (pH 7.5), 150 NaCl, 1 EDTA, 1 EGTA, 1% Triton X-100, 2.5 sodium pyrophosphate, 1 β-glycerophosphate, 1 Na3VO4, 20 NaF, and 1% protease inhibitor cocktail and phosphatase inhibitor (Roach) and kept at 4 °C for 40 min before debris was removed by centrifugation at 14,000×*g* for 10 min. Synaptosomal protein lysate was prepared by using an extraction kit for synaptic proteins (87793, Pierce). For Nifedipine treatment experiments, brain slices (prepared as described in the "Slice Electrophysiology" section) were incubated with 10 µM Nifedipine in the oxygen saturated ACSF for 1 h and then homogenized with the above protein lysis buffer. The protein samples were mixed with 25% volume of 5× SDS loading buffer (250 mM Tris–HCl, 10% SDS, 0.5% bromophenol blue, 50% glycerol, 5% beta-mercaptoethanol, pH 7.4) for electrophoresis on a SDS-PAGE ployacrylamide gel and electrotransfered to a PVDF filter. The filter was then blocked with 5% dry milk in TBST (20 mM Tris–HCl, 9% NaCl, 1% Tween-20, pH 7.6) and incubated overnight at 4 °C with primary antibodies in TBST. Following washing and incubation with appropriate secondary antibodies, the filter was washed extensively and developed using an enhanced chemiluminescence (Thermo) method of detection and analyzed using the AlphaEaseFC software as per manufacturer's instruction. The amount of total protein loaded was controlled by normalizing each tested protein with anti-actin immunoreactivity on the same blot.

Statistical Methods

All the data in the graphs were presented as mean ± SEM and statistically evaluated by independent-samples *t* tests. $p < 0.05$ was considered as significant (*$p < 0.05$, **$p < 0.01$, ***$p < 0.001$).

Results and Discussion

Increased Presynaptic RRP Size in APP KO Mice

Previous studies using cultured neurons showed that the readily releasable pool (RRP) size is increased in APP KO mice compared to wild type (WT) littermates [30]. To determine whether this alteration occurs in hippocampal slices, we used high concentration (500 mM) sucrose puffs to the Schaffer collateral area of acute hippocampal slices and recorded excitatory postsynaptic current (EPSC) in the CA1 pyramidal neurons (Fig. 1a). As shown in Fig. 1b, the application of sucrose evoked a significantly greater postsynaptic responses in APP KO compared to WT slices. These results suggest that the size of the RRP is greater in APP KO mice and that APP normally acts as a negative regulator of the RRP.

Elevated Synaptic Depletion in Response to High Frequency Stimulation in APP KO Mice

At presynaptic terminals, the reserve pool (RP) is thought to be important to replenish the RRP under intense neuronal activities [31, 32]. Therefore, we examined whether the size of the RP is altered in APP KO mice using high frequency stimulation. We recorded evoked EPSC from CA1 pyramidal neuron in response to a 5 Hz stimulation (lasting 180 s). As shown in Fig. 2a and b, both WT and APP KO mice showed

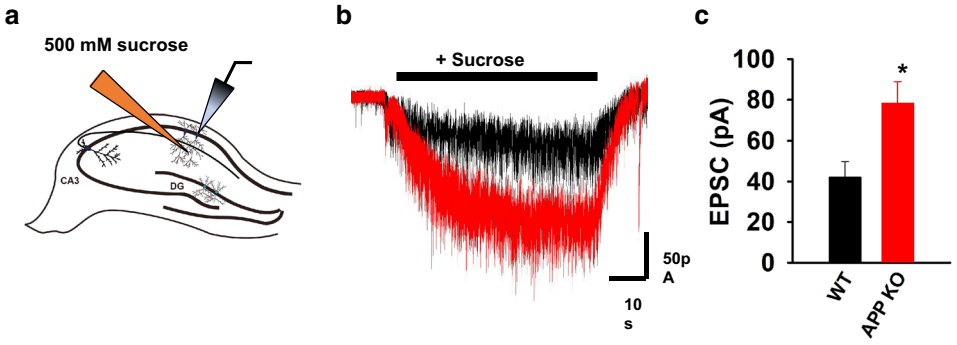

Fig. 1 Enhanced EPSC induced by high concentration sucrose in APP KO mice. **a** Sucrose application and whole-cell recordings in acute hippocampal slices. **b** Sample traces of 500 mM sucrose-induced EPSC responses recorded from CA1 neurons in WT (black) and APP KO (red) mice. **c** Summary graph of the sucrose-induced EPSC peak values (WT: 41.98 ± 7.79 pA, n = 8 [4]; APP KO: 78.30 ± 10.66 pA, n = 10 [5], p = 0.018). In all slice recording experiments (Figs. 1, 2, 3, 5), n represents number of slices. The number of mice is indicated in the bracket following the n

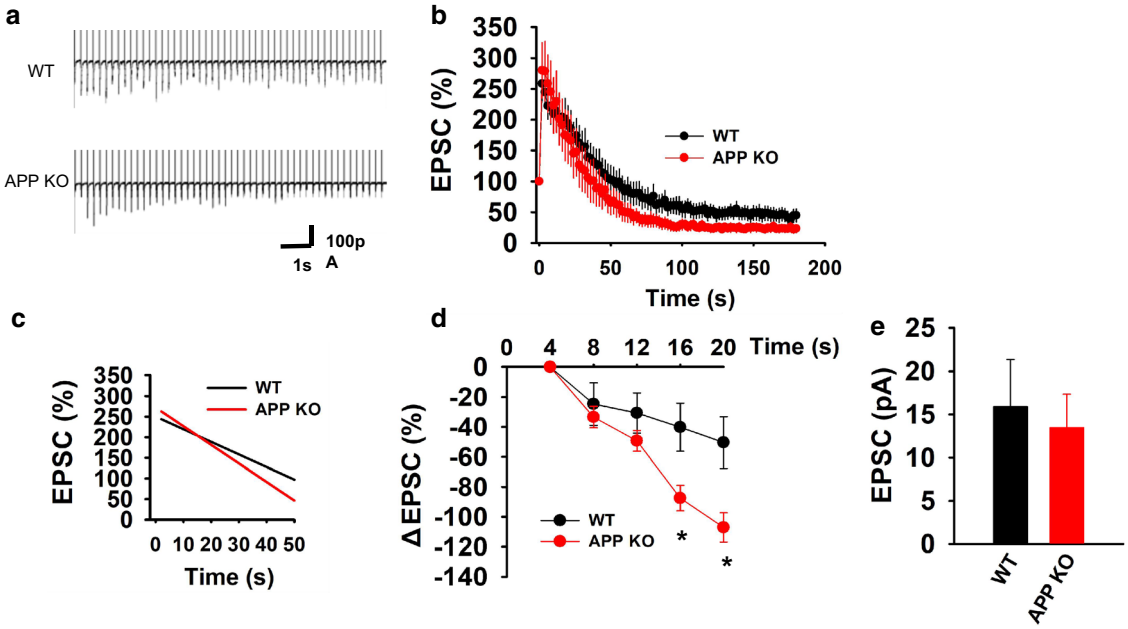

Fig. 2 Faster synaptic depletion in response to high frequency stimulation in APP KO mice. **a** Sample traces of EPSC responses during 5 Hz stimulation (180 s) in WT and APP KO CA1 neurons. **b** Summary graph of normalized EPSC responses during the course of 180 s of 5 Hz stimulation. **c** Descending liner fitting curves of EPSC in WT and APP KO during the first 2–50 s of 5 Hz stimulation period (WT: y = 249.97–3.05x, APP KO: y = 271.72–4.50x). **d** Summary graph of ΔEPSC values during the first 4–20 s of 5 Hz stimulation (the 16th second: WT: − 40.21 ± 16.08, n = 10 [5], APP KO: − 87.49 ± 8.51, n = 7 [4], p = 0.037; the 20th second: WT: − 50.34 ± 17.27, n = 10 [5], APP KO: − 107.05 ± 9.84, n = 7 [4], p = 0.023). **e** Summary graph of absolute EPSC amplitudes during the last 10 s of synaptic depletion (WT: 15.90 ± 5.46 pA, n = 7 [4]; APP KO: 13.47 ± 3.87 pA, n = 7 [4], p = 0.723)

initial facilitation followed by gradual depression of EPSCs. However, in APP KO slices, the depression was significantly faster and stabilized to a lower level compared to WT control (Fig. 2c, d) although the absolute amplitude of EPSCs was similar between genotypes (Fig. 2e). These results suggest that the size of the RP is reduced and/or its trafficking to the RRP is altered in APP KO mice. Thus APP deletion has opposing effects on the RRP and RP, suggesting that APP may play an important role in the dynamic regulation between these two pools of synaptic vesicles at the excitatory synapse.

Enhanced Synaptic depletion at Inhibitory Synapses in APP KO Mice

In addition to excitatory synapses, APP has also been implicated in presynaptic release at inhibitory synapses [33]. Therefore, we also examined inhibitory postsynaptic currents (IPSC) in response to sucrose application and 5 Hz stimulation in APP KO mice. As shown in Fig. 3a and b, sucrose induced an outward current that was significantly enhanced in APP KO slices. In response to 5 Hz stimulation the IPSC amplitude decreased gradually in both WT and KO groups, but the depression was significantly greater in APP KO compared to WT mice (Fig. 3c–e). These results suggest that APP may play a general role in modulating vesicle dynamics at both excitatory and inhibitory synapses.

Increased Phosphorylated Synapsins in APP KO Mice

Synapsins (Syn) are a family of presynaptic proteins known to be involved in the regulation of dynamic transition of synaptic vesicles between RP to RRP via a phosphorylation-dependent pathway [32, 34]. They are also implicated in vesicles priming and fusion at the presynaptic membrane [35, 36]. To investigate whether the effect of APP deletion is related to synapsins, we examined the level of phosphorylated synapsin 1 in APP KO mice. As shown in Fig. 4a and b, while the total synapsin 1 was not altered, the amount of phosphorylated synapsin 1 at serine 9 [p-Syn (Ser 9)] was significantly increased in APP KO compared to WT mice. To determine whether this change occurred at the synapse, we analyzed p-Syn1 (Ser 9) using synaptosomal protein lysates and found that the level of p-Syn1 (Ser 9) was also significantly higher in APP KO compared to WT mice (Fig. 4c and d). Since synapsin 2 is also involved in synaptic release and is potentially linked to APP [37–39], we also analyzed the level of p-Syn2 and found that it was significantly higher in APP KO mice (Fig. 4e). Previous studies have shown that synapsins can be phosphorylated by Ca^{2+}/calmodulin—dependent protein kinase II (CaMKII) [40, 41]; therefore we analyzed the activity of CaMKII. We found that the level of phosphorylated CaMKII (Thr 286), which is often used as an indicator of active CaMKII, was significantly higher in APP KO compared to WT mice (Fig. 4f). Immunostaining experiments of hippocampal sections also showed that the level of p-Syn1 (Ser 9) was higher in the CA1 area in APP KO mice (Fig. 4g). These results indicate that APP deletion enhances synapsin phosphorylation and/or inhibits synapsin dephosphorylation, suggesting that the effect of APP on vesicle dynamics may be mediated through phosphorylation/dephosphorylation of synapsins.

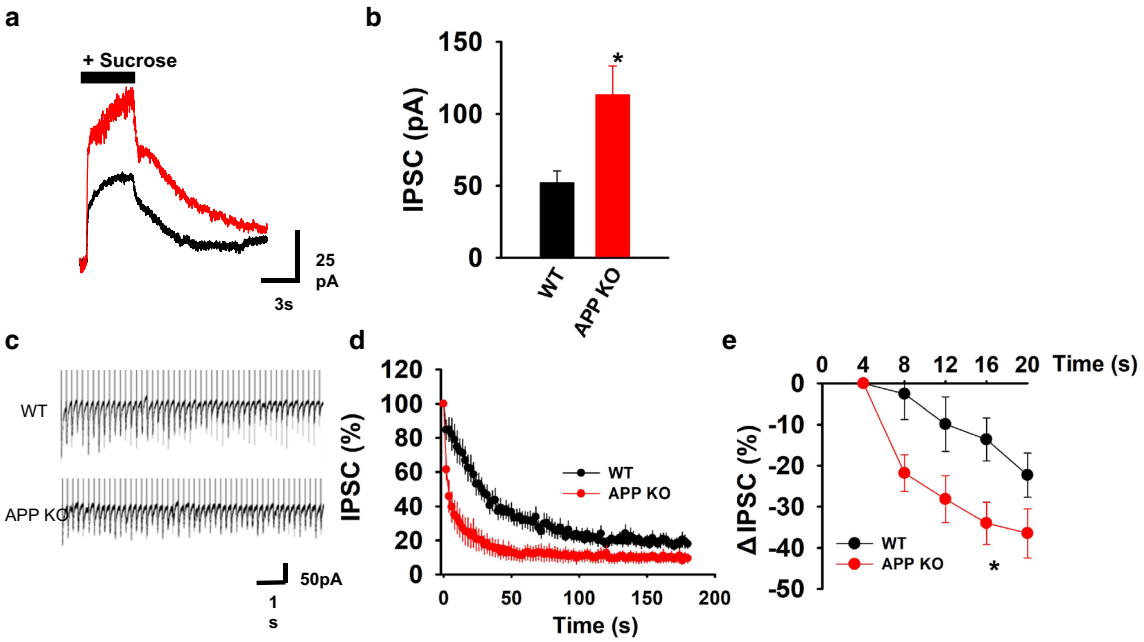

Fig. 3 Increased sucrose induced IPSC and faster synaptic depletion at inhibitory synapses in APP KO mice. **a** Sample traces of 500 mM sucrose induced IPSC responses recorded from CA1 neurons in WT and APP KO CA1 neuron. **b** Summary graph of sucrose induced IPSC peak value (WT: 52.05 ± 8.23 pA, n = 10 [5]; APP KO: 113.11 ± 20.24 pA, n = 11 [6], p = 0.014). **c** Sample traces of IPSC responses in response to 5 Hz stimulation (180 s) in WT and APP KO CA1 neurons. **d** Summary graph of normalized IPSC responses during the course of 180 s of 5 Hz stimulation. **e** Summary graph of ΔIPSC values during the first 4–20 s of 5 Hz stimulation (the 16th second: WT: − 13.60 ± 5.24, n = 7 [4], APP KO: − 34.02 ± 5.13, n = 9 [5], p = 0.016)

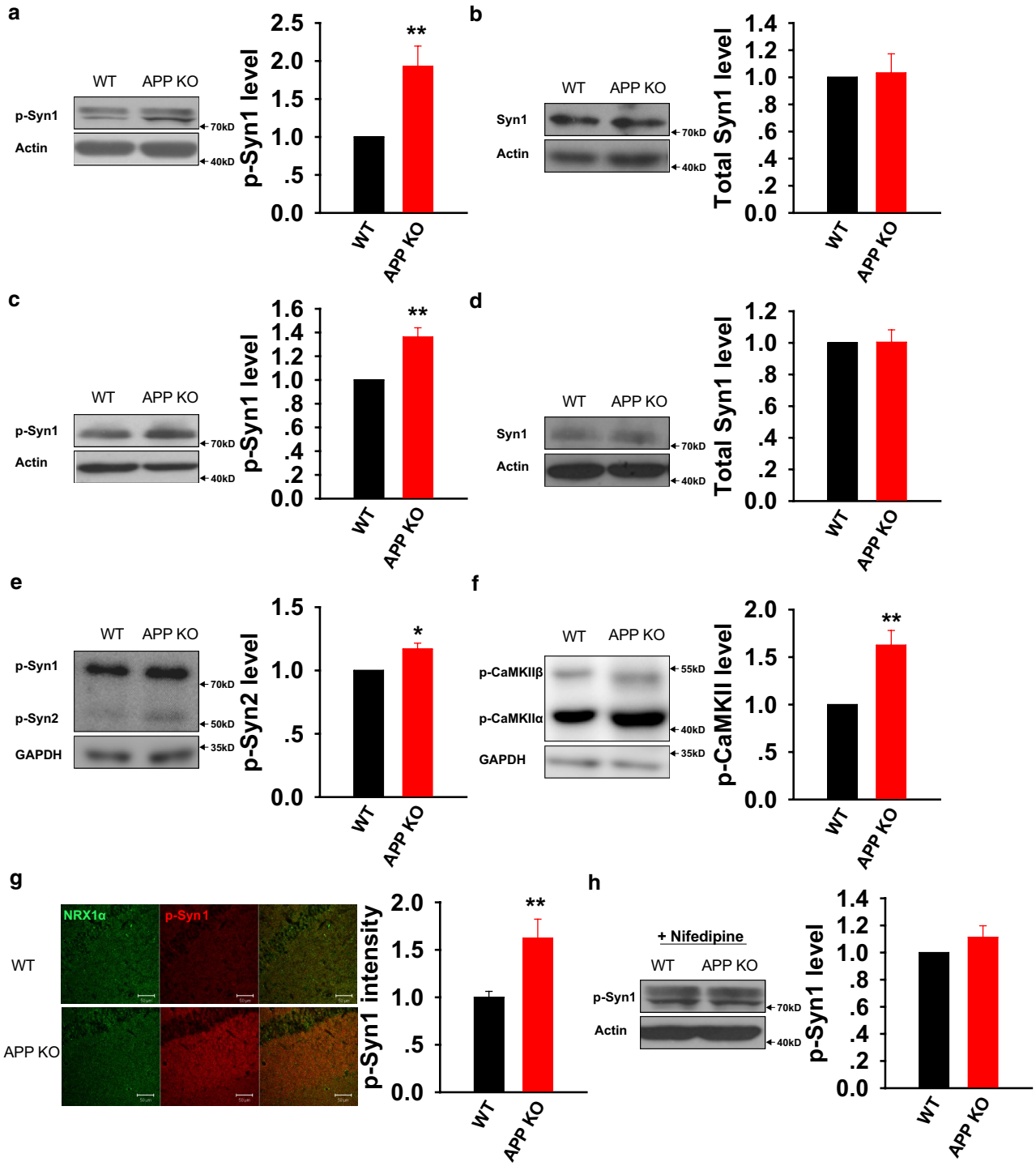

Rescue of p-Syn (Ser 9) and Synaptic depletion by Inhibiting L-Type Calcium Channels

Previous studies have shown that the level of L type calcium channel (LTCC) was increased in APP KO mice and this increase was responsible for the presynaptic changes at the GABAergic synapse in these mice [42]. Previous studies have also shown that synapin phosphorylation is associated with Ca^{2+} influx [43, 44]. Therefore, we reasoned that the increased p-Syn1 (Ser 9) in APP KO mice might also be related to the increased LTCC and subsequent Ca^{2+} influx. To test this hypothesis, we treated brain slices with the LTCC blocker nifedipine and then analyzed p-Syn1 (Ser 9). As the shown in Fig. 4h, the level of p-Syn1 (Ser 9)

◂**Fig. 4** Elevated levels of phosphorylated synapsins in APP KO mice. **a** Sample Western blots of total brain lysates and summary graph of p-Syn1 (Ser 9) level (WT: 1.00±0.00, n=6, APP KO: 1.93±0.27, n=6, p=0.006). **b** Sample Western blots of total brain lysates and summary graph of total synapsin 1 (WT: 1.00±0.00, n=5, APP KO: 1.03±0.14, n=5, p=0.833). **c** Sample Western blots of synaptosomal protein lysate and summary graph of p-Syn1 (Ser 9) (WT: 1.00±0.00, n=4, APP KO: 1.36±0.16, n=4, p=0.004). **d** Sample Western blots of synaptosomal protein lysate and summary graph of total Syn1 (WT: 1.000±0.000, n=3, APP KO: 1.00±0.08, n=3, p=0.968). **e** Sample blots and summary graph of p-Syn2 level in brain lysate (WT: 1.00±0.00, n=4; APP KO: 1.17±0.05, n=4, p=0.013). **f** Sample blots and summary graph of p-CaMKII (Thr 286) level in brain lysate (WT: 1.00±0.00, n=4; APP KO: 162±0.16, n=4, p=0.007). **g** Sample images of immunostained hippocampal sections (CA1 area) and summary graph of p-Syn1 (Ser 9) immunofluorescence intensity (WT: 1.00±0.19, n=9, APP KO: 1.62±0.20, n=9, p=0.009). **h** Sample Western blots of total protein lysates prepared from brain slices treated with nifedipine (WT: 1.00±0.00, n=4, APP KO: 1.11±0.09, n=4, p=0.233). n represents the number of mice in **a**–**f** and **h**, and the number of images from three pairs of animals

became similar between WT and APP KO slices. We then tested whether the elevated synaptic depletion in APP KO mice was also caused by altered LTCC function by treating brain slices with nifedipine. As shown in Fig. 5a–f, APP KO and WT slices now exhibited a similar degree of synaptic depression. It is important to note that in WT mice the depression in the presence of nifedipine appeared to be greater compared to that without the drug treatment (Fig. 2), suggesting an effect on WT rather than on APP KO mice. This could be due to an effect on basal synaptic transmission as nifedipine also increased basal synaptic responses in both WT and APP KO mice (Fig. 5g–i), and consequently the degree of depression was actually over estimated after the nifedipine treatment. Taken together, these results suggest that the effect of APP on synaptic depletion during high frequency stimulation is mediated by LTCC and subsequent Ca^{2+}-dependent phosphorylation of synapsins.

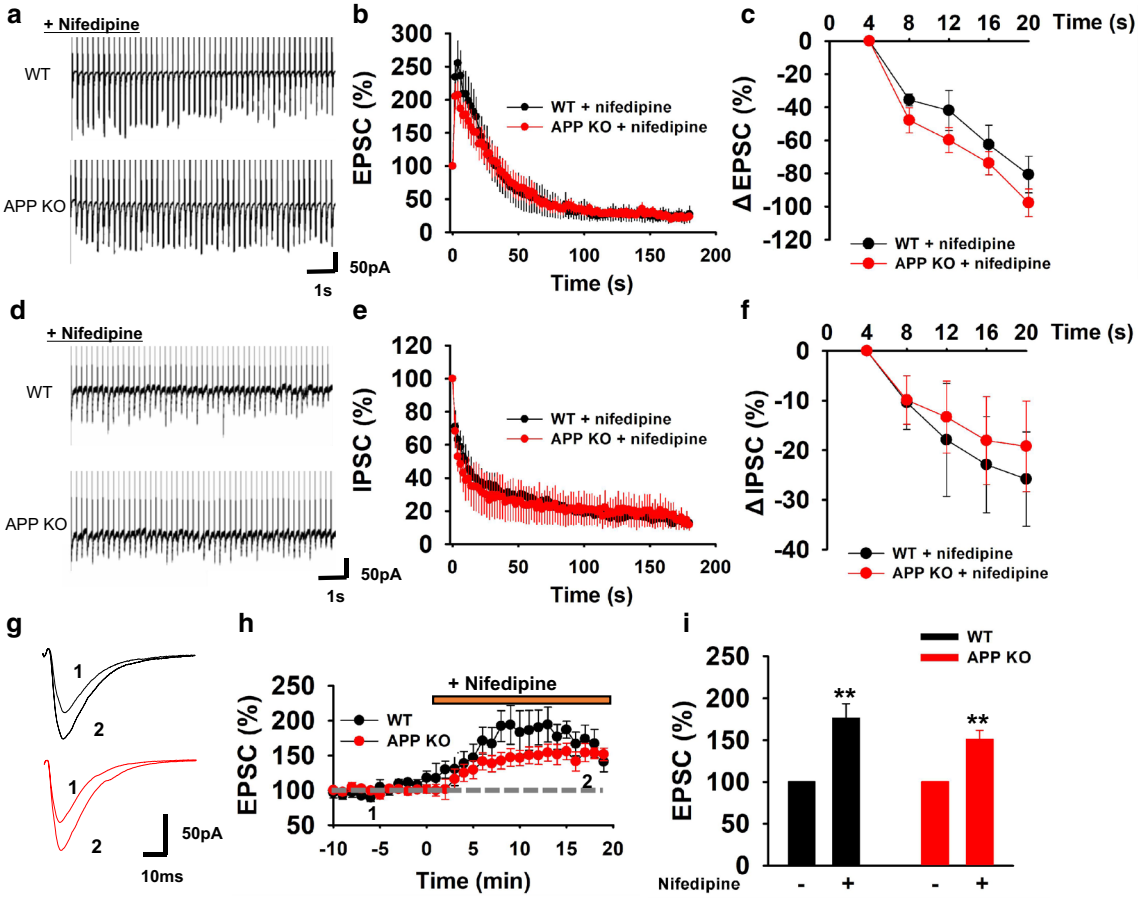

Fig. 5 Nifedipine slows down synaptic depletion in APP KO mice. **a, d** Sample traces of EPSC **a** and IPSC **d** responses during 5 Hz stimulation in nifedipine-treated WT and APP KO CA1 neurons. **b** and **e** Summary graphs of normalized EPSC (**b**) and IPSC (**e**) response during the course of 180 s of 5 Hz stimulation in nifedipine-treated slices. **c, f** Summary graphs of ΔEPSC (**c**) and ΔIPSC (**f**) values during the first 4–20 s of 5 Hz stimulation (**c**; 16th second: WT: − 62.57±11.70, n=6 [4]; APP KO: − 73.77±7.03, n=6 [4], p=0.431; 20th second: WT: − 80.71±11.12, n=6 [4]; APP KO: − 97.75±8.37, n=6 [4], p=0.249. **f**; 16th second: WT: − 22.91±9.70, n=5 [3]; APP KO: − 18.04±8.83, n=5 [3], p=0.720). **g** Sample traces EPSC responses before and during nifedipine treatment in WT and APP KO CA1 neuron. (**h, i**) Summary graph of normalized EPSC responses before and during nifedipine treatment (WT before: 100.00±0.00, n=6 [4]; during: 176.58±17.08, n=6 [4], p=0.001. APP KO before: 100.00±0.00, n=5 [3]; during: 150.81±11.09, n=5 [3], p=0.001)

In summary, by using a combination electrophysiological recordings and biochemical analyses, we have demonstrated that APP KO mice have a larger RRP and faster synaptic depletion during high frequency stimulation. These synaptic changes are associated with increased levels of phosphorylated synapsins. Although previous elegant studies have shown alterations in the abundance of presynaptic proteins in APP single and conditional APP/APLP2 double knockout mice [45, 46], specific changes in synapsins and their regulation by protein phosphorylation have not been demonstrated. Our findings in synapsins may be of particular relevance because these proteins are thought to play a key role in synaptic depletion in response to sustained high frequency stimulation. Changes in synaptic depletion observed in this study may also contribute to synaptic deficits, such as LTP found in APP KO mice. It is possible that during high frequency stimulation, which is typically used to trigger LTP, faster synaptic depletion may affect the degree of postsynaptic depolarization and therefore impair LTP. Another important finding of the present study is that both synapsins and synaptic depletion can be rescued by inhibiting LTCC, extending a previous study showing that APP directly interacts with LTCC and regulates GABA release [42]. Therefore, our results suggest that APP maintains a proper RP/RRP size through suppression of L type calcium channels, activation of CaMKII and subsequent synapsin phosphorylation. Future studies would be to determine whether other kinases and phosphatases, such as PKA [47], are involved in synapsin phosphorylation/dephosphorylation in the context of APP regulation and whether manipulations of synapsins can rescue the behavioral deficits in APP KO mice. Elucidation of the APP-synapsin pathway would open a new avenue of investigation that may ultimately help understand the role of APP at the synapse and provide potential targets to treat AD.

Acknowledgements We thank all members of Jia lab for their technical assistance and comments on the manuscript.

Funding This work was supported by Grants from the Canadian Institutes of Health Research (CIHR, MOP119421, ZPJ), Canadian Natural Science and Engineering Research Council (NSERC, RGPIN341498, ZPJ), Natural Science Foundation of China (NSFC 31200805, ZZ), NSFC and CIHR Joint Health Research Initiative Program (81161120543, WX and CCI117959, ZPJ), National Postdoctoral Program for Innovative Talents (1131000,047, AL) and Brain Canada (ZPJ).

References

1. Shankar GM, Li S, Mehta TH, Garcia-Munoz A, Shepardson NE, Smith I, Brett FM, Farrell MA, Rowan MJ, Lemere CA, Regan CM, Walsh DM, Sabatini BL, Selkoe DJ (2008) Amyloid β-protein dimers isolated directly from alzheimer brains impair synaptic plasticity and memory. Nat Med 14:837
2. Schmechel DE, Saunders AM, Strittmatter WJ, Crain BJ, Hulette CM, Joo SH, Pericak-Vance MA, Goldgaber D, Roses AD (1993) Increased amyloid β-peptide deposition in cerebral cortex as a consequence of apolipoprotein e genotype in late-onset Alzheimer disease. Proc Natl Acad Sci USA 90:9649–9653
3. Mckhann GM, Knopman DS, Chertkow H, Hyman BT Jr, Kawas CH, Jack CR, Klunk WE, Koroshetz WJ, Manly JJ, Mayeux R (2011) The diagnosis of dementia due to Alzheimer's disease: recommendations from the National Institute on Aging-Alzheimer's Association workgroups on diagnostic guidelines for Alzheimer's disease. Alzheimers Dement 7:263–269
4. Kamenetz F, Tomita T, Hsieh H, Seabrook G, Borchelt D, Iwatsubo T, Sisodia S, Malinow R (2003) APP processing and synaptic function. Neuron 37:925
5. Nilsberth C, Westlinddanielsson A, Eckman CB, Condron MM, Axelman K, Forsell C, Stenh C, Luthman J, Teplow DB, Younkin SG (2001) The 'Arctic' APP mutation (E693G) causes Alzheimer's disease by enhanced A|[beta]| protofibril formation. Nat Neurosci 4:887
6. Oddo S, Caccamo AShepherd JD, Murphy MP, Golde TE, Kayed R, Metherate R, Mattson MP, Akbari Y, Laferla FM (2003) Triple-transgenic model of Alzheimer's disease with plaques and tangles: intracellular Abeta and synaptic dysfunction. Neuron 39:409–421
7. Szodorai A, Kuan YH, Hunzelmann S, Engel U, Sakane A, Sasaki T, Takai Y, Kirsch J, Müller U, Beyreuther K (2009) APP anterograde transport requires Rab3A GTPase activity for assembly of the transport vesicle. J Neurosci 29:14534–14544
8. Sabo SL, Ikin AF, Buxbaum JD, Greengard P (2003) The amyloid precursor protein and its regulatory protein, FE65, in growth cones and synapses in vitro and in vivo. J Neurosci 23:5407–5415
9. Cheung HN, Dunbar C, Mórotz GM, Cheng WH, Chan HY, Miller CC, Lau KF (2014) FE65 interacts with ADP-ribosylation factor 6 to promote neurite outgrowth. FASEB J 28:337–349
10. Magara F, Wolfer DP (1999) Genetic background changes the pattern of forebrain commissure defects in transgenic mice underexpressing the β-amyloid-precursor protein. Proc Natl Acad Sci USA 96:4656-4661
11. Osterhout JA, Stafford BK, Nguyen PL, Yoshihara Y, Huberman AD (2015) Contactin-4 mediates axon-target specificity and functional development of the accessory optic system. Neuron 86:985–999
12. Olsen O, Kallop DY, Mclaughlin T, Huntwork-Rodriguez S, Wu Z, Duggan CD, Simon DJ, Lu Y, Easley-Neal C, Takeda K (2014) Genetic analysis reveals that amyloid precursor protein and death receptor 6 function in the same pathway to control axonal pruning independent of β-secretase. J Neurosci 34:6438–6447
13. Tyan SH, Shih AY, Walsh JJ, Maruyama H, Sarsoza F, Ku L, Eggert S, Hof PR, Koo EH, Dickstein DL (2012) Amyloid precursor protein (APP) regulates synaptic structure and function. Mol Cel Neurosci 51:43
14. Weyer SW, Zagrebelsky M, Herrmann U, Hick M, Ganss L, Gobbert J, Gruber M, Altmann C, Korte M, Deller T (2014) Comparative analysis of single and combined APP/APLP knockouts reveals reduced spine density in APP-KO mice that is prevented by APPsα expression. Acta Neuropathol Commun 2:36
15. Perez R, Zheng H, Der Ploeg LHTV, Koo EH (1997) The β-Amyloid precursor protein of Alzheimer's disease enhances neuron viability and modulates neuronal polarity. J Neurosci 17:9407–9414
16. Matrone C, Luvisetto S, La Rosa LR, Tamayev R, Pignataro A, Canu N, Yang L, Barbagallo APM, Biundo F, Lombino F (2012) Tyr682 in the Aβ-precursor protein intracellular domain

regulates synaptic connectivity, cholinergic function, and cognitive performance. Aging Cell 11:1084–1093
17. Hick M, Herrmann U, Weyer SW, Mallm JP, Tschäpe JA, Borgers M, Mercken M, Roth FC, Draguhn A, Slomianka L (2015) Acute function of secreted amyloid precursor protein fragment APPsα in synaptic plasticity. Acta Neuropathol 129:161–162
18. Lee KJ, Moussa CE, Lee Y, Sung Y, Howell BW, Turner RS, Pak DT, Hoe HS (2010) Beta amyloid-independent role of amyloid precursor protein in generation and maintenance of dendritic spines. Neuroscience 169:344–356
19. Terry RD, Masliah E, Salmon DP, Butters N, Deteresa R, Hill R, Hansen LA, Katzman R (1991) Physical basis of cognitive alterations in Alzheimer's disease: synapse loss is the major correlate of cognitive impairment. Ann Neurol 30:572
20. De SB, Karran E (2016) The cellular phase of Alzheimer's disease. Cell 164:603
21. Ring S, Weyer SW, Kilian SB, Waldron E, Pietrzik CU, Filippov MA, Herms J, Buchholz C, Eckman CB, Korte M (2007) The secreted β-Amyloid precursor protein ectodomain APPsα is sufficient to rescue the anatomical, behavioral, and electrophysiological abnormalities of APP-deficient mice. J Neurosci 27:7817–7826
22. Dawson GR, Seabrook GR, Zheng H, Smith DW, Graham S, O'Dowd G, Bowery BJ, Boyce S, Trumbauer ME, Chen HY (1999) Age-related cognitive deficits, impaired long-term potentiation and reduction in synaptic marker density in mice lacking the beta-amyloid precursor protein. Neuroscience 90:1–13
23. Zou C, Sophie C, Stephane M, Elena M, Carmelo S, Yuan S, Song S, Zhu K, Dorostkar MM, Müller UC (2016) Amyloid precursor protein maintains constitutive and adaptive plasticity of dendritic spines in adult brain by regulating D-serine homeostasis. Embo J 35:2213–2222
24. Fanutza T, Del PD, Ford MJ, Castillo PE, D'Adamio L (2015) APP and APLP2 interact with the synaptic release machinery and facilitate transmitter release at hippocampal synapses. Elife Sci 4:e09743
25. Zheng H, Jiang M, Trumbauer ME, Sirinathsinghji DJS, Hopkins R, Smith DW, Heavens RP, Dawson GR, Boyce S, Conner MW (1995) Beta-Amyloid precursor protein-deficient mice show reactive gliosis and decreased locomotor activity. Cell 81:525–531
26. Meng Y, Zhang Y, Tregoubov V, Janus C, Cruz L, Jackson M, Lu W-Y, MacDonald JF, Wang JY, Falls DL (2002) Abnormal spine morphology and enhanced LTP in LIMK-1 knockout mice. Neuron 35:121–133
27. Jia Z, Agopyan N, Miu P, Xiong Z, Henderson JT, Gerlai R, Taverna FA, Velumian AA, Macdonald JF, Carlen PL (1996) Enhanced LTP in mice deficient in the AMPA receptor GluR2. Neuron 17:945–956
28. Zhou Z, Hu J, Passafaro M, Xie W, Jia Z (2011) GluA2 (GluR2) regulates metabotropic glutamate receptor-dependent long-term depression through N-cadherin-dependent and cofilin-mediated actin reorganization. J Neurosci 31:819–833
29. Liu A, Zhou Z, Dang R, Zhu Y, Qi J, He G, Leung C, Pak D, Jia Z, Xie W (2016) Neuroligin 1 regulates spines and synaptic plasticity via LIMK1/cofilin-mediated actin reorganization. J Cell Biol 212:449–463
30. Priller C, Bauer T, Mitteregger G, Krebs B, Kretzschmar HA, Herms J (2006) Synapse formation and function is modulated by the amyloid precursor protein. J Neurosci 26:7212–7221
31. Pyle JL, Kavalali ET, Piedras-Rentería ES, Tsien RW (2000) Rapid reuse of readily releasable pool vesicles at hippocampal synapses. Neuron 28:221–231
32. Rizzoli SO and Betz WJ (2005) Synaptic vesicle pools. Nat Rev Neurosci 6:57–69
33. Seabrook GR, Smith DW, Bowery BJ, Easter A, Reynolds T, Fitzjohn SM, Morton RA, Zheng H, Dawson GR, Sirinathsinghji DJ (1999) Mechanisms contributing to the deficits in hippocampal synaptic plasticity in mice lacking amyloid precursor protein. Neuropharmacology 38:349–359
34. Chi P, Greengard P, Ryan TA (2003) Synaptic vesicle mobilization is regulated by distinct synapsin i phosphorylation pathways at different frequencies. Neuron 38:69–78
35. Esser L, Wang CR, Hosaka M, Smagula CS, Südhof TC, Deisenhofer J (1998) Synapsin I is structurally similar to ATP-utilizing enzymes. Embo J 17:977–984
36. Hosaka M, Südhof TC (1998) Synapsins I and II are ATP-binding proteins with differential Ca^{2+} regulation. J Biol Chem 273:1425–1429
37. Song SH, Augustine GJ (2015) Synapsin Isoforms and Synaptic Vesicle Trafficking. Mol Cell 38:936–940
38. Medrihan L, Cesca F, Raimondi A, Lignani G, Baldelli P, Benfenati F (2013) Synapsin II desynchronizes neurotransmitter release at inhibitory synapses by interacting with presynaptic calcium channels. Nat Commun 4:1512
39. Laßek M, Weingarten J, Einsfelder U, Brendel P, Müller U, Volknandt W (2013) Amyloid precursor proteins are constituents of the presynaptic active zone. J Neurochem 127:48–56
40. White RR, Kwon Y, Taing M, Lawrence DS, Edelman AM (1998) Definition of optimal substrate recognition motifs of Ca^{2+}-calmodulin-dependent protein kinases IV and II reveals shared and distinctive features. J Biol Chem 273:3166–3172
41. Leenders AGM, Sheng ZH (2005) Modulation of neurotransmitter release by the second messenger-activated protein kinases: implications for presynaptic plasticity. Pharmacol Ther 105:69–84
42. Yang L, Wang Z, Wang B, Justice NJ, Zheng H (2009) Amyloid precursor protein regulates Cav1.2 L type calcium channel levels and function to influence GABAergic short-term plasticity. J Neurosci 29:15660–15668
43. Kennedy MB, Greengard P (1981) Two calcium/calmodulin-dependent protein kinases, which are highly concentrated in brain, phosphorylate protein I at distinct sites. Proc Natl Acad Sci USA 78:1293-1297
44. Dolphin AC, Greengard P (1981) Neurotransmitter- and neuromodulator-dependent alterations in phosphorylation of protein I in slices of rat facial nucleus. J Neurosci 1:192–203
45. Laßek M, Weingarten J, Ackerpalmer A, Bajjalieh SM, Muller U, Volknandt W (2014) Amyloid precursor protein knockout diminishes synaptic vesicle proteins at the presynaptic active zone in mouse brain. Curr Alzheimer Res 11:971
46. Laßek M, Weingarten J, Wegner M, Mueller B, Rohmer M, Baeumlisberger D, Arrey TN, Hick M, Ackermann J, Ackerpalmer A (2016) APP Is a context-sensitive regulator of the hippocampal presynaptic active zone. PLoS Comput Biol 12:4
47. Menegon A, Bonanomi D, Albertinazzi C, Lotti F, Ferrari G, Kao HT, Benfenati F, Baldelli P, Valtorta F (2006) Protein kinase A-mediated synapsin I phosphorylation is a central modulator of Ca^{2+}-dependent synaptic activity. J Neurosci 26:11670–11681